CHEMISTRY
A EUROPEAN JOURNAL

DOI: 10.1002/chem.201000607

Conformational Structure and Energetics of 2-Methylphenyl(2′-methoxyphenyl)iodonium Chloride: Evidence for Solution Clusters

Yong-Sok Lee,*[a] Milan Hodošček,[b] Joong-Hyun Chun,[c] and Victor W. Pike[c]

Abstract: Diaryliodonium salts allow the efficient incorporation of cyclotron-produced [^{18}F]fluoride ions into electron-rich and electron-deficient arenes to provide potential radiotracers for molecular imaging in vivo with positron emission tomography (PET). This process ($ArI^+Ar' + {}^{18}F^- \rightarrow Ar{}^{18}F + Ar'I$) is still not well understood mechanistically. To better understand this and similar reactions, it would be valuable to understand the structures of diaryliodonium salts in organic media, where the reactions are typically conducted. In this endeavor, the X-ray structure of a representative iodonium salt, 2-methylphenyl(2′-methoxyphenyl)iodonium chloride (**1**), was determined. Our X-ray structure analysis showed **1** to have the conformational *M–P* dimer as the unit cell with hypervalent iodine as a stereogenic center in each conformer. With the ab initio replica path method we constructed the inversion path between the two enantiomers of **1**, thereby revealing two additional pairs of enantiomers that are likely to undergo fast interconversion in solution. Also LC–MS of **1** showed the presence of dimeric and tetrameric anion-bridged clusters in weak organic solution. This observation is consistent with the energetics of **1**, both as monomeric and dimeric forms in MeCN, calculated at the B3LYP/DGDZVP level. These evidences of the existence of dimeric and higher order clusters of **1** in solution are relevant to achieve a deeper general understanding of the mechanism and outcome of reactions of diaryliodonium salts in organic media with nucleophiles, such as the [^{18}F]fluoride ion.

Keywords: cluster compounds · dimerization · iodinium salts · inversion pathways · stereogenic iodine

Introduction

Diaryliodonium salts (ArI^+ArX^-) widely serve as useful reagents for arylation and oxidation reactions.[1] They are also becoming very useful substrates for the preparation of fluorine-18-labeled ($t_{1/2} = 109.7$ min) fluoroarenes as potential radiotracers for biomedical imaging with positron emission tomography (PET).[2] In view of these increasing synthetic applications, a detailed understanding of the structure of diaryliodonium salts in organic solution is desirable to assist in understanding reaction mechanisms and outcomes.

Previous studies have shown that diaryliodonium salts are in general fully dissociated in aqueous or polar media,[3] but have also suggested that they may exist as ion pairs or dimeric structures in less polar organic solvents.[3,4] Solid-state structures determined with X-ray crystallography often prove diaryliodonium salts to be anion-bridged dimers held together by iodine–halogen bonds.[5] However, correspondence between solid-state and solution structure has not been elucidated previously. Here, we present X-ray crystallography data on an example of an unsymmetric diaryliodonium salt, 2-methylphenyl(2′-methoxyphenyl)iodonium chloride (**1**). Interestingly, these data unveiled hypervalent iodine as

[a] Dr. Y.-S. Lee
Center for Molecular Modeling
Division of Computational Bioscience
Center for Information Technology, National Institutes of Health
Department of Health and Human Services, Building 12A
Room 2049, Bethesda, MD 20892 (USA)
Fax: (+1) 301-402-2867
E-mail: leeys@mail.nih.gov

[b] Dr. M. Hodošček
National Heart, Lung and Blood Institute
National Institutes of Health
Department of Health and Human Services
Bethesda, MD 20892 (USA)
and
National Institute of Chemistry, Ljubljana (Slovenia)

[c] Dr. J.-H. Chun, Dr. V. W. Pike
Molecular Imaging Branch, National Institute of Mental Health
National Institutes of Health
Department of Health and Human Services
Room B3 C346A, Building 10, 10 Center Drive,
Bethesda, MD 20892 (USA)

Supporting information for this article is available on the WWW under http://dx.doi.org/10.1002/chem.201000607.

a previously unrecognized stereogenic center within a dimeric structure, composed of conformational *M* and *P* enantiomers (Scheme 1). An immediate consequence of the stereogenic iodine is the possible racemization of **1** in solution. In the present work, this racemization process was investigated with quantum chemistry at the B3LYP/DGDZVP level. For this purpose, we utilized the ab initio replica path (RPATH) method[6,7] to construct the inversion path for the conformers *M* and *P* of **1**. This method readily identifies the transition state (TS) of a chemical reaction or conformational change of interest without prior knowledge of the TS geometry, as exemplified in our previous study of the inversion of 1,4-benzodiazepines.[7] We also found mass spectrometric evidence for solution clusters of **1**, and therefore, quantum chemical calculations were carried out to probe the existence of dimeric **1** in MeCN, choosing the latter as a representative organic solvent.

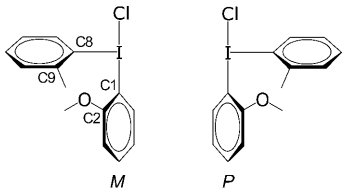

Scheme 1. *M* and *P* are conformational enantiomers of **1** and are defined, respectively, for the negative and positive Cl-I-C8-C9 (ϕ_1) dihedral angle.

Results and Discussion

X-ray structure and interconversion of the conformational enantiomers of 1: Our X-ray study found **1** to have the *M*–*P* dimer as the unit cell in a centrosymmetric crystal (Figure 1). In particular, the central iodine atoms of the *M* and *P* enantiomers are located above (7.6°) and below (−7.6°) the plane defined by C1-C8-Cl, respectively, as measured by their improper dihedral angles I-C1-C8-Cl, and therefore, show that the hypervalent iodine of **1** is stereogenic. A similar observation has been made for the sulfur of phenyl *p*-tolyl sulfoxide, which is known to racemize by pyramidal inversion.[8] Aside from the presence of a stereogenic iodine atom, the structure of **1** resembles those of Ph_2I–Z (Z = Cl, Br, or I)[5] in that **1** forms a bridged dimer whose iodine coordination is square planar. One difference, however, is that the methoxy and methyl substituents render the chloride bridge in **1** longer and more asymmetric (I–Cl = 3.101 and 3.028 Å) than in Ph_2I–Cl (I–Cl = 3.065, 3.105 Å). The I–Cl bonds in **1** are primarily ionic since their lengths are about 0.64 Å longer than in solid $PhICl_2$ (2.46 Å).[9] It is this ionicity that allows the secondary bonds[10] to arise, so enabling the crystallization of **1** as the Cl-bridged dimer.

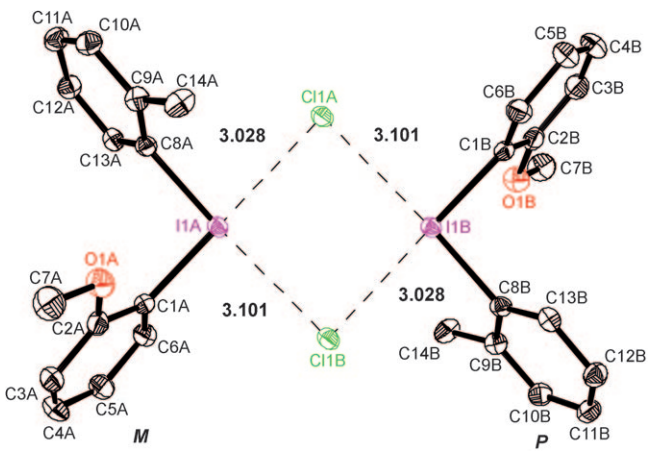

Figure 1. X-ray crystal structure of dimeric **1**, represented in an ORTEP drawing (50% thermal ellipsoids with hydrogen atoms omitted for clarity). Some bond distances [Å] are indicated. Atoms labeled with A and B belong to the *M* and *P* monomers, respectively.

In our theoretical study, we first probed the racemization of **1** in the gas phase. The resulting potential energy surface (PES) obtained from the RPATH method is shown in Figure 2; the inset is a graphical representation of the 60 replicas that are superimposed with the best fit by using the six atoms (C1–C6) of the anisyl group of *M*1 as the common docking point. The PES shown in Figure 2 gives three distinct conformers of *M* and *P*, as well as two TSs that are best described by the rotation around two torsion angles, Cl-I-C8-C9 (ϕ_1) and C8-I-C1-C2 (ϕ_2), as shown in Figure 3. Note that the states shown in Figures 2 and 3 are approximate since geometry at each replica was minimized with an added harmonic penalty function. The conformer *M*2 is 2.2 kcal mol^{-1} more stable than *M*1 due to less steric repulsion between the two aryl rings, achieved through an equatorial rotation of the tolyl group (ϕ_2) with respect to the anisyl group. Further rotation of the tolyl group gives rise to

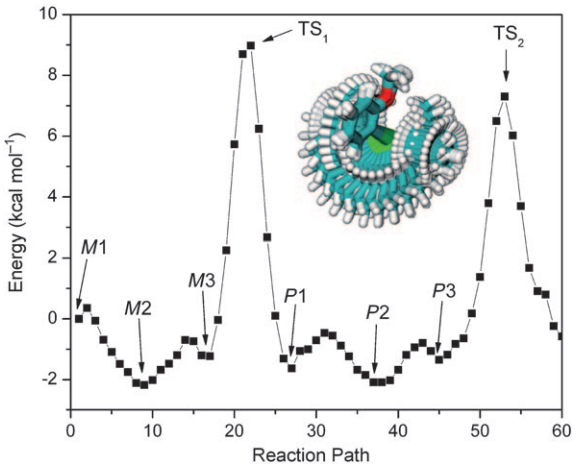

Figure 2. PES for the inversion of **1** in the gas phase calculated with the RPATH method by using 60 replicas. Energy at each point, without zero point vibration and thermal contribution, is relative to *M*1. Arrows indicate the approximate states. Inset: Graphical representation of the 60 replicas. Individual structures are superimposed with the best fit by using the six atoms (C1–C6) of the anisyl group of *M*1 as the common docking point.

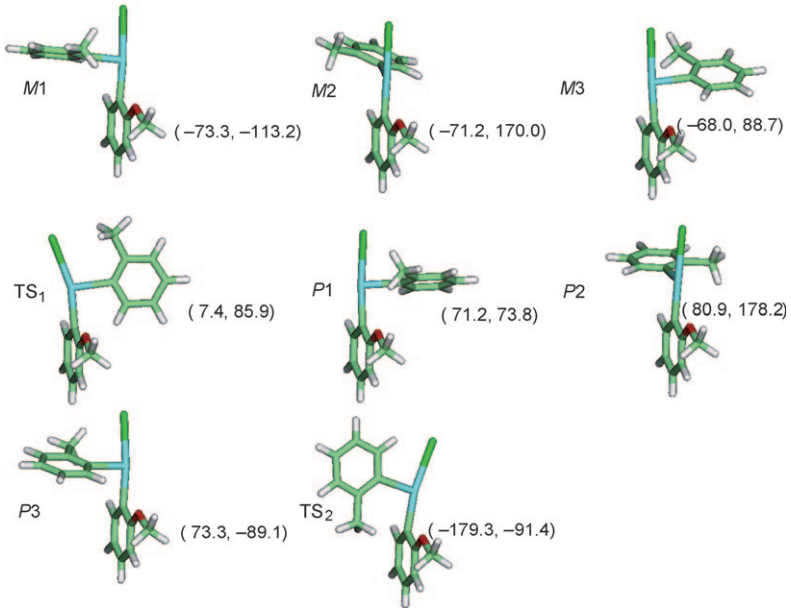

Figure 3. Conformers of *M* and *P*, and of the two TSs. Values in parenthesis indicate the torsion angles, Cl-I-C8-C9 (ϕ_1) and C8-I-C1-C2 (ϕ_2); see Scheme 1 for atom numbering.

another conformer *M*3, which is 1.2 kcal mol^{-1} more stable than *M*1. At TS_1, the ionic I–Cl bond (2.82 Å) is longer than in *M*1 (2.75 Å) due to steric repulsion between the tolyl group and the Cl atom; this weakening of the I–Cl bond in TS_1 is reflected in the greater energy of 9.0 kcal mol^{-1} of TS_1 relative to *M*1. Further rotation of ϕ_1 yields the conformer *P*1, a pseudo enantiomer of *M*1. Counter-clockwise rotation of the tolyl ring gives rise to *P*2 and *P*3, the respective pseudo enantiomers of *M*2 and *M*3. The energy of TS_2 is 1.6 kcal mol^{-1} lower than that of TS_1 due to the Cl atom being *anti* to the tolyl methyl group. The calculated energy barriers within the conformers of *M* or *P* are no higher than 2.6 kcal mol^{-1}, indicating that their interconversion at room temperature likely occurs on a picosecond timescale.

The geometries of the approximate states in Figure 3 were further optimized with Gaussian 03 utilizing the polarized continuum model with the UAKS parameters set in MeCN.[11] Single imaginary frequencies for the vibrational–torsional motion of the tolyl group in the direction of *M*3 or *P*1 through TS_1 (−36.6 cm^{-1}) and of *P*3 or *M*1 through TS_2 (−39.4 cm^{-1}) were obtained, but none in any other conformers. In terms of energetics (Table 1), *M*1 and *M*3 are essentially isoenergetic, whereas *M*2 is only 0.7 kcal mol^{-1} more stable than either of these, due to the attenuated steric repulsion in MeCN. The inclusion of the solvent effect lengthened the ionic bond I–Cl in *M*1 from 2.75 Å in vacuum to 2.87 Å in MeCN, and in TS_1 from 2.82 Å in vacuum to 3.08 Å in MeCN. It also rendered TS_1 and TS_2 isoenergetic at 9.1 kcal mol^{-1} higher than *M*1, suggesting that the inversion of **1** occurs equally well through the enantiomeric TS_1 or TS_2 (not calculated), as in the case of benzodiazepines.[7] The energy barrier of 9.1 kcal mol^{-1} further suggests that the racemization at room temperature in MeCN occurs in the microsecond range, which is too fast to be investigated with NMR spectroscopy. In these circumstances, a theoretical approach, such as RPATH, seems the only viable way for studying the geometry of diaryliodonium salts and their energetics in organic solvents.

The superposition of the fully optimized structures onto the six atoms (C1–C6) of the anisyl group of *M*1 as the common docking point gives a visual representation of each of the conformer pairs (Figure 4): the pairs *M*1 and *P*1, *M*2 and *P*2, and *M*3 and *P*3 are enantiomers, whereas TS_1 and TS_2 are not. These optimized structures further provide detailed information on the iodine inversion

Table 1. Calculated energies and geometrical parameters of the conformers and TSs of **1**, as shown in Figure 3, in MeCN at the B3LYP/DGDZVP level.

Structure	Energy[a] relative to *M*1 [kcal mol^{-1}]	ϕ_1 Cl-I-C8-C9 [°]	ϕ_2 C8-I-C1-C2 [°]	I–Cl [Å]
*M*1	0	−70.9	−73.2	2.87
*M*2	−0.7	−77.2	173.6	2.87
*M*3	−0.05	−76.3	82.4	2.86
TS_1	9.1 (−36.6 cm^{-1})[b]	−2.6	87.2	3.08
*P*1	0	71.0	73.3	2.87
*P*2	−0.8	77.4	−173.7	2.87
*P*3	−0.03	76.1	−82.6	2.86
TS_2	9.1 (−39.4 cm^{-1})[b]	179.2	−88.0	3.01

[a] Energies include the zero-point correction as well as the enthalpy and the entropy contribution at 298.15 K. [b] Imaginary torsional–vibrational mode of the tolyl group.

for each enantiomeric pair. Figure 5 shows the microscopic iodine inversion of *M*1 to *P*1 wherein the central iodine atoms of *M*1 and *P*1 are located above (2.0°) and below (−2.0°) the plane of C1-C8-Cl, respectively. These calculated improper dihedral angles are 5.6° smaller than those found in the X-ray structure of **1**. On the *M*1–TS_1–*P*1 path, the iodine of *M*1 first moves downwards with respect to the C1-C8-Cl plane until the *M*3 state is reached; the iodine then moves upwards to reach TS_1, and downwards again to complete the inversion. The *P*1–TS_2–*M*1 path shows an opposite movement of the iodine atom, but this is not symmetric to the *M*1–TS_1–*P*1 path by inversion, because TS_1 and TS_2 are not enantiomers.

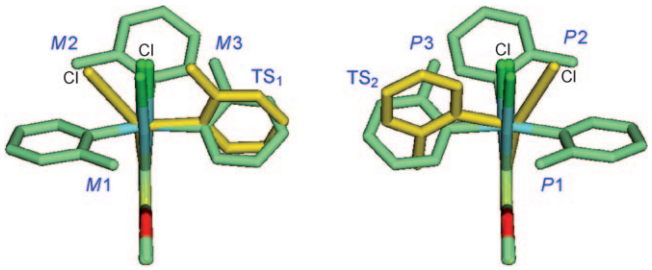

Figure 4. Overlay of the fully geometry-optimized *M* and *P* conformers (green) and transition states (yellow) by using the six atoms (C1–C6) of the anisyl group of *M*1 as common docking point. The root mean square deviation (rmsd) of each fit to *M*1 is less than 0.07 Å. Each of the pairs of *M*1–*P*1, *M*2–*P*2 and *M*3–*P*3 is enantiomeric. The Cl atoms of TS_1 and TS_2 do not align with those of *M* or *P* due to steric repulsion with the tolyl group. Hydrogen atoms are not shown.

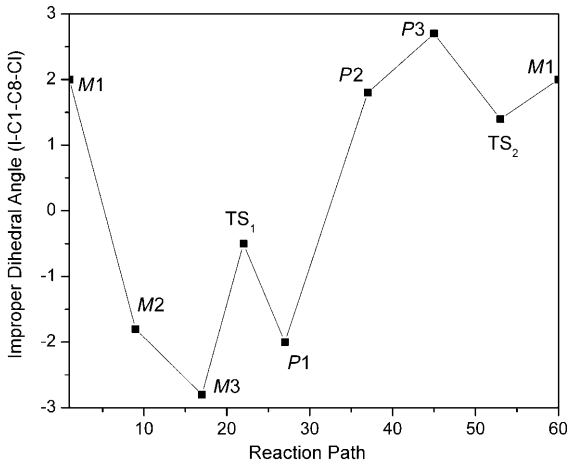

Figure 5. Variation of the improper dihedral angle I-C1-C8-Cl along the reaction path shows the inversion of the iodine atom during racemization; the central iodine atom of the *M*1 and *P*1 pair is located above (2.0°) and below (−2.0°) the plane of C1-C8-Cl, respectively.

Evidence for clusters of 1 from LC–MS, MS, and energetics calculations: During the characterization of **1** in MeCN by LC–MS, we encountered the unexpected finding that reversed phase LC operated with water/methanol/acetic acid as mobile phase gave not a single sharp peak but a broad multi-peaked elution profile starting from elution near the solvent front (capacity factor, $k' \approx 1.0$) up to capacity factors of ≈4 (see the Supporting Information). MS of all material in this broad elution range gave a base peak at *m*/*z* 324.9, corresponding to the monomeric cation of **1**, $[C_{14}H_{14}OI]^+$. Close scrutiny of these spectra also showed a set of low abundance ions beginning at *m*/*z* 684.3 and another set at *m*/*z* 708.3. The former set, according to its isotope [*M*] and [*M*+2] abundance ratio, contained one Cl atom, whereas the latter did not. The ion *m*/*z* 684.3 was deduced to be the Cl-bridged dimer $[(MeOC_6H_4IMeC_6H_4)_2Cl]^+$, uniquely generated from an unseen Cl-bridged tetrameric metastable ion with composition $[(MeOC_6H_4IMeC_6H_4)_4Cl_2+H]^{2+}$. High resolution mass spectrometry confirmed the elemental composition of the detected dimeric ion, $[(MeOC_6H_4IMeC_6H_4)_2Cl]^+$ (see the Supporting Information). Similarly, the ion at *m*/*z* 708.3 was deduced to be an acetate-bridged dimer $[(MeOC_6H_4IMeC_6H_4)_2OAc]^+$ uniquely generated from an unseen acetate-bridged tetrameric metastable ion with composition $[(MeOC_6H_4IMeC_6H_4)_4OAc+H]^{2+}$ (see the Supporting Information). Incorporation of OAc^- into the latter must have occurred in the HPLC mobile phase. These observations directly show the existence of stable dimeric and tetrameric clusters of **1** even in the weakly organic HPLC mobile phase. How might such clusters form?

As listed in Table 1, the six conformers of **1** are comparable in energy and thus, all are likely to exist in MeCN at room temperature. These conformers could then form a dimer in organic solvent through secondary bonding interactions[10] that were attributed to be the driving force for formation of the dimeric solid-state structure. To investigate this possibility, quantum chemical calculations were performed on the three pairs of enantiomers. Each dimer was constructed by manually putting their geometry-optimized monomers together. Calculations were also performed on an *M*1–*M*1 dimer for comparison. These calculations indicate that in MeCN the *M*1–*P*1 heterodimer is more stable than *M*1–*M*1 and *M*3–*P*3 by 1.8 kcal mol^{-1} and 2.6 kcal mol^{-1}, respectively; the *M*2–*P*2 dimer converged to the *M*3–*P*3 dimer.

Figure 6 illustrates the energy-minimized structures of *M*1–*P*1 and *M*1–*M*1 in MeCN. The dimer *M*1–*P*1 closely resembles the X-ray structure shown in Figure 1 as evidenced

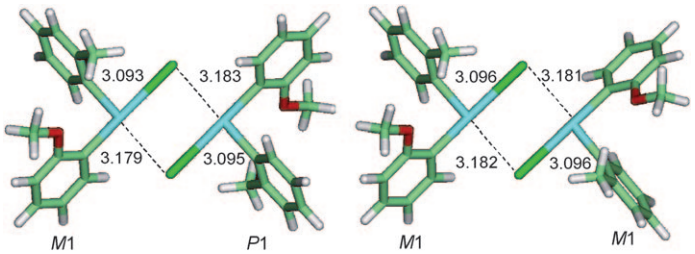

Figure 6. Geometry-optimized dimers *M*1–*P*1 and *M*1–*M*1 of **1** in MeCN. In *M*1–*P*1, the 2-methyl and 2′-methoxy groups of *M*1 are pointing out of the plane, whereas those of *P*1 are pointing into the plane. In the *M*1–*M*1 dimer, all substituents are pointing out of the plane.

by the rmsd of 0.02 Å between the experimental and calculated bond distances and the less than 3° difference in bond angles (Table 3 in the Supporting Information). The calculated I–Cl distances (3.09, 3.18 Å) in *M*1–*P*1 are longer than the ones in monomeric *M*1 or *P*1 (2.87 Å) but are comparable to those observed in the crystal structure (3.03, 3.10 Å). When *M*1 approaches *P*1 or vice versa, the Mulliken atomic charge on the iodine atom (+0.38) of *M*1 forms a strong charge interaction with the negative charge on the chlorine atom (−0.70) of *P*1 to form another ionic bond with a length of 3.18 Å. This charge interaction in turn polarizes

the I–Cl bond of the monomers *M*1 and *P*1 as manifested by an increase in length from 2.87 to 3.09 Å. In line with this bond lengthening, the calculations showed a further polarization of the atomic charge on I (+0.44) and Cl (−0.71) in the *M*1–*P*1 dimer relative to those in the *M*1 or *P*1 monomer. Note that these atomic charges are comparable to other electrostatic potential-derived charges such as CHelpG.[11]

With the zero-point energy correction and thermal enthalpy contribution at 298.15 K, the ΔH for dimerization of *M*1–*P*1 in MeCN, calculated by subtracting the sum of the energy of each monomer from the energy of the *M*1–*P*1 dimer, was $-9.0\,\mathrm{kcal\,mol^{-1}}$. When the entropy contribution was included, ΔG for the dimerization became $+2.8\,\mathrm{kcal\,mol^{-1}}$. This is primarily due to the loss of the translational and rotational (TR) entropy of the two monomers upon dimerization, which is $91\,\mathrm{cal\,mol^{-1}\,K^{-1}}$ or about $46\,R$ based on the ideal gas approximation. However, the TR entropy contribution of a solute to dimerization is known to be much lower in the liquid phase because of hindered movement. For example, the experimental TR entropy contribution to the dimerization of a protein in aqueous solution has been reported to be $5\pm4\,R$, as opposed to $50\,R$ estimated from the ideal gas approximation.[12] Assuming the high end of the TR entropy (i.e., $9\,R$), the ΔG for the dimerization of *M*1 and *P*1 was estimated to be $-13.1\,\mathrm{kcal\,mol^{-1}}$ at 298.15 K. The basis set superposition error for *M*1–*P*1 formation in the gas phase was only $1.4\,\mathrm{kcal\,mol^{-1}}$ and thus, was unlikely to affect the calculated thermochemical stability of *M*1–*P*1 in MeCN. These results taken together, suggest that **1** predominantly exists as dimers in MeCN. The thermochemical stability of tetramers has not been considered due to lack of structural information. Nonetheless, the LC–MS study indicates the existence of tetramers of **1** in solution. This might be driven by an increase in entropy of solvent molecules surrounding the more structurally ordered tetramers. Further experimental and theoretical efforts are needed to better explain the formation and stability of higher order clusters.

Besides being more stable than *M*1–*M*1 and *M*3—*P*3, the *M*1–*P*1 heterodimer has a negligible dipole moment ($\mu=0.07$ D). As a result, the dipole–dipole interaction among *M*1–*P*1 dimers is minimal compared to *M*1–*M*1 ($\mu=0.82$ D) or *M*3–*P*3 ($\mu=0.37$ D). This may explain the formation of the *M*1–*P*1 dimer as a unit cell in a centrosymmetric crystal. In the case of *M*1–*M*1 or *M*3—*P*3 dimers (not observed), the unit cell might require doubling or even quadrupling in size to minimize the overall dipole moment of the crystal.

The favorable dimerization energy calculated here, further indicates that well-known reactions of diaryliodonium salts similar to **1** with nucleophiles in organic solvents may require the dissociation of dimers or possibly even tetramers. In the case of the increasingly useful radiofluorination reactions,[2] such dissociation will likely be necessary to allow replacement of chloride ions with ^{18}F ions, preceding attack of the bound fluoride ion onto an aryl carbon atom to give either of the two possible [^{18}F]fluorarene products.[13] We are now using the RPATH method to locate the transition state of such fluorination reactions:

$$(\mathrm{ArI^+Ar'Cl^-})_2 \rightarrow \mathrm{ArI^+Ar'Cl^-} \xrightarrow{^{18}F^-} \mathrm{Ar^{18}F/Ar'^{18}F + Ar'I/Ar}$$

Conclusion

The determination of the X-ray structure of **1** unveiled hypervalent iodine acting as a stereogenic center. In addition, with the ab initio RPATH method, we have identified two additional enantiomers not observed in the crystal structure of **1**, as well as two TSs for the inversion of the enantiomers. This inversion has a calculated energy barrier of $9.1\,\mathrm{kcal\,mol^{-1}}$ in MeCN, and proceeds with an equatorial rotation of the 2-tolyl group with respect to the 2′-anisyl group, together with an internal rotation of the 2-tolyl group. Finally, our quantum chemical calculations suggest that **1** likely exists as dimers in MeCN because of the strong secondary bonding interaction between the I and the Cl atoms of the *M* and *P* forms of **1**. These calculations appear consistent with LC–MS observations of clusters of **1** in weak organic solution. Taken together, these findings now help our continuing studies of the radiofluorination of iodonium salts to produce radiotracers for molecular imaging with PET.

Experimental Section

Synthesis of 1: 2-Methylphenyl(2′-methoxyphenyl)iodonium chloride (**1**) was synthesized by treating 2-methoxyphenyl boronic acid with 2-[hydroxy(tosyloxy)iodo]toluene[14] followed by anion metathesis of the generated diaryliodonium tosylate with ammonium chloride.

X-ray crystallography of 1: Crystals of **1** were grown from MeCN by portionwise addition of water at room temperature. X-ray data were collected by using a SMART Apex CCD diffractometer (Bruker, Madison, WI, USA) with graphite-monochromated $Mo_{K\alpha}$ radiation ($\lambda=0.71073$ Å). Crystal data for **1**: $C_{14}H_{14}ClIO$, $M_r=360.60$, triclinic, $P\bar{1}$, $T=100(2)$ K, $a=7.593(3)$ Å, $b=9.491(4)$ Å, $c=10.383(5)$ Å, $V=697.5(5)$ Å^3, $Z=2$, $\mu(Mo_{Ka})=2.469\,\mathrm{mm^{-1}}$, 5554 reflections collected, 2764 unique ($R_{ini}=0.0321$), GOF = 1.043, final $R_1(I>2\sigma(I))=0.0304$, $wR_2=0.0774$. CCDC-710484 (**1**) contains the supplementary crystallographic data for this paper. These data can be obtained free of charge from The Cambridge Crystallographic Data Centre via www.ccdc.cam.ac.uk/data_request/cif.

Quantum chemistry: To investigate the racemization of **1**, 60 replicas were constructed by combining two sets of 30 replicas in a cyclic pathway. First, 30 replicas were constructed by interpolation between the geometry-minimized *M* and *P* enantiomers of **1**, starting from their X-ray structures, and then another 30 replicas between *P* and *M*. Energy minimization, utilizing CHARMM[15] interfaced with GAMESS,[16] was then performed on each replica with an added harmonic penalty function to restrain distances in root-mean square space between adjacent replicas along the reaction pathway in the form:

$$E_{\mathrm{rms}} = \frac{1}{2}\sum_{i=1}^{N-1} K_{\mathrm{rms}}(R_{i,i+1} - \langle R\rangle)^2 \qquad (1)$$

where N is the number of replicas i along the pathway, K_{rms} is the force constant (set here to $10^3\,\mathrm{kcal\,mol^{-1}\,A^2}$), and $R_{i,i+1}$ and $<R>$ are rmsd values given by:

$$R^2_{i,j+1}\sum_{j=1}^{n} w_j = \sum_{j=1}^{n} w_j[(x_j^{(i)} - x_j^{(i+1)})^2 + (y_j^{(i)} - y_j^{(i+1)})^2 + (z_j^{(i)} - z_j^{(i+1)})^2]$$
$$\langle R\rangle = N^{-1}\sum_{i=1}^{N-1} R_{i,j+1} \quad (2)$$

where n is the total number of replicated atoms j with coordinates ($x_j^{(k)}$, $y_j^{(\ )}$, $z_j^{(k)}$) in replica k, and w_j is a suitable input-defined parameter. Accordingly, the penalty function is proportional to the difference in the rmsd between the two neighboring structures. In addition, an angle energy term [Eq. (3)], was included to prevent merging between the adjacent points (force constants $K_{\text{angle}} = 100$ and cosmax = 0.95).

$$E_{\text{angle}} = \frac{1}{2}\sum_{i=1}^{N-1} K_{\text{angle}}((R^2_{i,j+2} - R^2_{i,j+1} - R^2_{i+1,j+2})/(2R_{i,j+1}R_{i+1,j+2}) - \cos\max)^2 \quad (3)$$

The average restraint energy shown in Equation (1) was less than 0.02 kcal mol^{-1} per replica after 200 steps of energy minimization. The ab initio program GAMESS was used for all RPATH calculations at the B3LYP/DGDZVP level. Further refinement of the approximate TS was carried out with the TS search algorithm by using the keywords, opt = (ts, calcfc, noeigentest), as implemented in Gaussian 03 software.[11]

Acknowledgements

This work was supported by the Intramural Research Program of the National Institutes of Health (NIMH and CIT). We are grateful to Dr. S. Hassan (CIT) for discussion, and Dr. M. J. Panzner (University of Akron) for X-ray analysis of **1**. The quantum chemical study utilized PC/LINUX clusters at the Center for Molecular Modeling of the NIH (http://cit.nih.gov). We are also deeply grateful to Dr. H. U. Shetty (NIMH) for assistance with LC–MS.

[1] a) P. J. Stang, V. V. Zhdankin, *Chem. Rev.* **1996**, *96*, 1123–1178; b) A. Varvoglis in *Hypervalent Iodine in Organic Synthesis*, Academic Press, London, **1997**; c) A. Varvoglis, S. Spyroudis, *Synlett* **1998**, 221–232; d) V. V. Zhdankin, P. J. Stang, *Chem. Rev.* **2002**, *102*, 2523–2584; e) M. Ochiai, *Top. Curr. Chem.* **2003**, *224*, 5–68; f) V. V. Zhdankin, P. J. Stang, *Chem. Rev.* **2008**, *108*, 5299–5358; g) E. A. Merritt, B. Olofsson, *Angew. Chem.* **2009**, *121*, 9214; *Angew. Chem. Int. Ed.* **2009**, *48*, 9052.

[2] a) V. W. Pike, F. I. Aigbirhio, *J. Chem. Soc. Chem. Commun.* **1995**, 2215–2216; b) R. Gail, C. Hocke, H. H. Coenen, *J. Labelled Compd. Radiopharm.* **1997**, *40*, 50–52; c) A. Shah, V. W. Pike, D. A. Widdowson, *J. Chem. Soc. Perkin Trans. 1* **1998**, 2043–2046; d) S. Martín-Santamaría, M. A. Carroll, C. M. Carroll, C. D. Carter, V. W. Pike, H. S. Rzepa, D. A. Widdowson, *Chem. Commun.* **2000**, 649–650; e) T. L. Ross, J. Emert, C. Hocke, H. H. Coenen, *J. Am. Chem. Soc.* **2007**, *129*, 8018–8025; f) M-R. Zhang, K. Kumata, K. Suzuki, *Tetrahedron Lett.* **2007**, *48*, 8632–8635; g) M. A. Carroll, J. Nairne, G. Smith, D. A. Widdowson, *J. Fluorine Chem.* **2007**, *128*, 127–132; h) L. Cai, S. Y. Lu, V. W. Pike, *Eur. J. Org. Chem.* **2008**, 2853–2873L; i) S. Telu, J. Chun, F. G. Siméon, S. Lu, V. W. Pike, *J. Labelled Compd. Radiopharm.* **2009**, *52*, S4.

[3] a) F. M. Beringer, M. Mausner, *J. Am. Chem. Soc.* **1958**, *80*, 4535–4536; b) Y. Yamada, K. Kashima, M. Okawara, *Polym. Lett. Ed.* **1976**, *14*, 65–71.

[4] a) N. P. Hacker, D. V. Leff, J. L. Dektar, *J. Org. Chem.* **1991**, *56*, 2280–2282; b) S. Martín-Santamaría, M. A. Carroll, V. W. Pike, H. S. Rzepa, D. A. Widdowson, *J. Chem. Soc. Perkin Trans. 2* **2000**, 2158–2161.

[5] a) N. W. Alcock, R. M. Countryman, *J. Chem. Soc. Dalton Trans.* **1977**, 217–219; b) N. W. Alcock, R. M. Countryman, *J. Chem. Soc. Dalton Trans.* **1987**, 193–196; c) H. Li, S. Jiang, *Acta Crystallogr. Sect. E* **2006**, *63*, o83–085; d) C.-Y. Liu, H. Li, A.-G. Meng, *Acta Crystallogr. Sect. E* **2007**, *63*, o3647.

[6] H. L Woodcock, M. Hodošček, P. Sherwood, Y. S. Lee, H. F. Schaefer III, B. R. Brooks, *Theor. Chem. Acc.* **2003**, *109*, 140–148.

[7] Y. S. Lee, V. W. Pike, M. Hodošček, *J. Phys. Chem. A* **2008**, *112*, 1604–1611.

[8] E. G. Miller, D. R. Rayner, H. T. Thomas, K. Mislow, *J. Am. Chem. Soc.* **1968**, *90*, 4861–4868.

[9] a) E. M. Archer, T. G. D. Van Schalkwyk, *Acta Crystallogr.* **1953**, *6*, 88–92; b) J. V. Carey, P. A. Chaloner, P. B. Hitchcock, T. Neugebauer, K. R. Seddon, *J. Chem. Res.* **1996**, *348*, 358–359.

[10] a) N. W. Alcock, *Adv. Inorg. Chem.* **1972**, *15*, 1–58; b) G. A. Landrum, N. Goldberg, R. Hoffman, R. M. Minyaev, *New J. Chem.* **1998**, *22*, 883–890.

[11] Gaussian 03, Revision D.01, M. J. Frisch, G. W. Trucks, H. B. Schlegel, G. E. Scuseria, M. A. Robb, J. R. Cheeseman, J. A. Montgomery, Jr., T. Vreven, K. N. Kudin, J. C. Burant, J. M. Millam, S. S. Iyengar, J. Tomasi, V. Barone, B. Mennucci, M. Cossi, G. Scalmani, N. Rega, G. A. Petersson, H. Nakatsuji, M. Hada, M. Ehara, K. Toyota, R. Fukuda, J. Hasegawa, M. Ishida, T. Nakajima, Y. Honda, O. Kitao, H. Nakai, M. Klene, X. Li, J. E. Knox, H. P. Hratchian, J. B. Cross, C. Adamo, J. Jaramillo, R. Gomperts, R. E. Stratmann, O. Yazyev, A. J. Austin, R. Cammi, C. Pomelli, J. W. Ochterski, P. Y. Ayala, K. Morokuma, G. A. Voth, P. Salvador, J. J. Dannenberg, V. G. Zakrzewski, S. Dapprich, A. D. Daniels, M. C. Strain, O. Farkas, D. K. Malick, A. D. Rabuck, K. Raghavachari, J. B. Foresman, J. V. Ortiz, Q. Cui, A. G. Baboul, S. Clifford, J. Cioslowski, B. B. Stefanov, G. Liu, A. Liashenko, P. Piskorz, I. Komaromi, R. L. Martin, D. J. Fox, T. Keith, M. A. Al-Laham, C Y. Peng, A. Nanayakkara, M. Challacombe, P. M. W. Gill, B. Johnson, W. Chen, M. W. Wong, C. Gonzalez, J. A. Pople, Gaussian, Inc., Wallingford CT, **2004**.

[12] Y. B. Yu, P. L. Privalov, R. S. Hodges, *Biophys. J.* **2001**, *81*, 1632–1642.

[13] J.-H. Chun, S. Y. Lu, Y.-S. Lee, V. W. Pike, *J. Org.Chem.* **2010**, *75*, 3332–3338.

[14] M. A. Carroll, V. W. Pike, D. A. Widdowson, *Tetrahedron Lett.* **2000**, *41*, 5393–5396.

[15] K. P. Eurenius, D. C. Chatfield, M. HodoŠček, R. R. Brooks, *Int. J. Quantum Chem.* **1996**, *60*, 1189–1200.

[16] M. W. Schmidt, K. K. Baldridge, J. A. Boatz, S. T. Elbert, M. S. Gordon, J. H. Jensen, S. Koseki, N. Matsunaga, K. A. Nguyen, S. Su, T. L. Windus, M. Dupuis, J. A. Montgomery, *J. Comput. Chem.* **1993**, *14*, 1347–1363.

Received: March 9, 2010
Published online: July 15, 2010

